

# Stability analyses of divergence and vorticity damping on gnomonic cubed-sphere grids

*Timothy C. Andrews, Christiane Jablonowski*

*Department of Climate and Space Sciences, University of Michigan*

*CESM Workshop, Boulder, Colorado*

*Monday 9<sup>th</sup> June 2025*

# Numerical diffusion

All dynamical cores require diffusion.

Implicit: Embedded in numerical methods

Explicit: Extra terms, e.g. in the horizontal momentum equations.

# Numerical diffusion

All dynamical cores require diffusion.

Implicit: Embedded in numerical methods

Explicit: Extra terms, e.g. in the horizontal momentum equations.

For explicit diffusion, there is a finite range of stability for the damping coefficient,  $C$ .

# Numerical diffusion

All dynamical cores require diffusion.

Implicit: Embedded in numerical methods

Explicit: Extra terms, e.g. in the horizontal momentum equations.

For explicit diffusion, there is a finite range of stability for the damping coefficient,  $C$ .

If  $C$  is too small: Energy at the small scales can cause instability

# Numerical diffusion

All dynamical cores require diffusion.

Implicit: Embedded in numerical methods

Explicit: Extra terms, e.g. in the horizontal momentum equations.

For explicit diffusion, there is a finite range of stability for the damping coefficient,  $C$ .

If  $C$  is too small: Energy at the small scales can cause instability

If  $C$  is too large: The diffusion causes instability

# Numerical diffusion

All dynamical cores require diffusion.

Implicit: Embedded in numerical methods

Explicit: Extra terms, e.g. in the horizontal momentum equations.

For explicit diffusion, there is a finite range of stability for the damping coefficient,  $C$ .

If  $C$  is too small: Energy at the small scales can cause instability

If  $C$  is too large: The diffusion causes instability

# Contents:

1. Divergence and vorticity damping
2. Cubed-sphere grids
3. Linear stability analysis
4. Application to CAM-FV3\*

\* CAM-FV3: NCAR Community Atmosphere Model (CAM), run with the finite-volume cubed-sphere (FV3) dynamical core.

# Explicit diffusion

Artificial diffusion of order  $2q$ , coefficient  $\nu$ :

Laplacian ( $q = 1$ ):  $\nu \nabla^2 \mathbf{u}$

Hyperviscosity ( $q \geq 2$ ):  $(-1)^{q+1} \nu \nabla^{2q} \mathbf{u}$ .

Horizontal momentum equations, for  $\mathbf{u} = (u, v, 0)$ :

$$\frac{\partial \mathbf{u}}{\partial t} = \dots + (-1)^{q+1} \nu \nabla^{2q} \mathbf{u}$$



# Divergence and vorticity damping

Instead, damp the divergent and rotational modes

$$\frac{\partial \mathbf{u}}{\partial t} = \dots + (-1)^{q+1} \nu_D \nabla(\nabla^{2(q-1)} D) \\ + (-1)^{q+1} \nu_\xi \nabla \times (\nabla^{2(q-1)} \xi \hat{\mathbf{k}}),$$

Divergence:  $D = \nabla \cdot \mathbf{u}$

Vorticity (relative):  $\xi = \hat{\mathbf{k}} \cdot (\nabla \times \mathbf{u})$ ,  $\hat{\mathbf{k}} = (0,0,1)$

# Divergence and vorticity damping

Instead, damp the divergent and rotational modes,

$$\frac{\partial \mathbf{u}}{\partial t} = \dots + (-1)^{q+1} \nu_D \nabla(\nabla^{2(q-1)} D) \\ + (-1)^{q+1} \nu_\xi \nabla \times (\nabla^{2(q-1)} \xi \hat{\mathbf{k}}),$$

Divergence:  $D = \nabla \cdot \mathbf{u}$

Vorticity (relative):  $\xi = \hat{\mathbf{k}} \cdot (\nabla \times \mathbf{u})$ ,  $\hat{\mathbf{k}} = (0,0,1)$

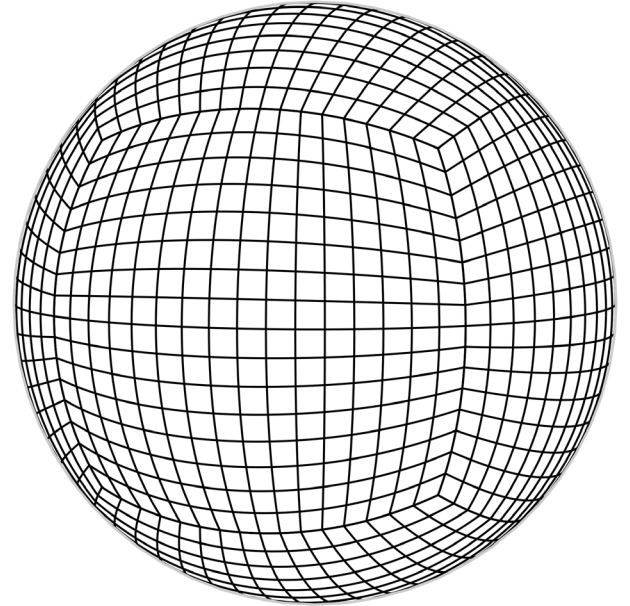
$$\frac{\partial D}{\partial t} = \dots + (-1)^{q+1} \nu_D \nabla^{2q} D,$$

$$\frac{\partial \xi}{\partial t} = \dots + (-1)^{q+1} \nu_\xi \nabla^{2q} \xi.$$

# Gnomonic cubed-sphere grids

Avoids the pole problem of lon-lat grids

Gnomonic: map straight lines from six panels (cube faces) onto great circles on the sphere



From Anthony Chen

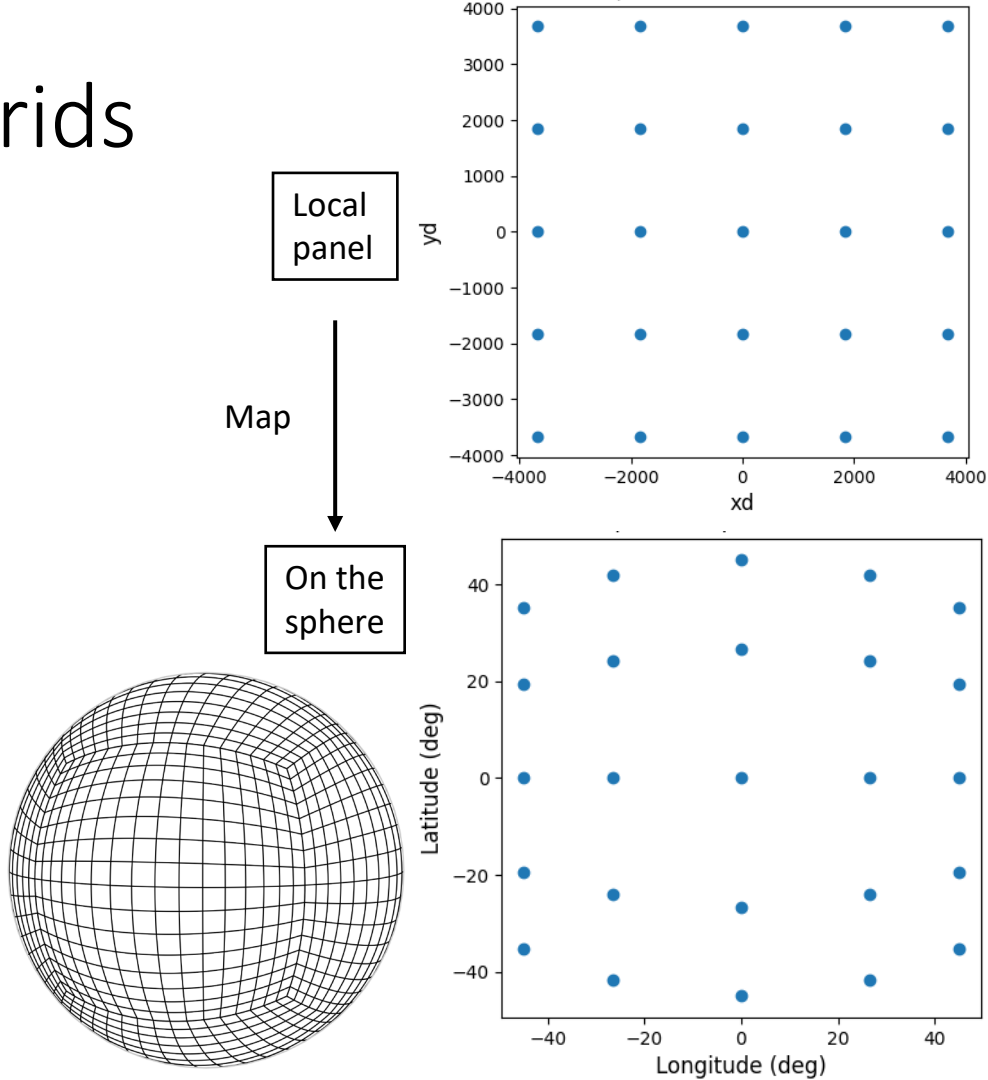
# Three cubed-sphere grids

## 1. **Equidistant**, original grid of Sadournay (1972):

- Equal spacings on the local panel  
= wide range of cell areas

## 2. **Equiangular** (Ronchi, 1995), most common, used by LFRic (UK Metoffice), SE (NCAR)

## 3. **Equi-edge**, an additional option (default) for FV3



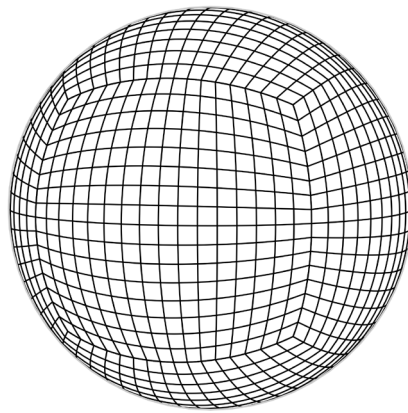
# Three cubed-sphere grids

1. **Equidistant**, original grid of Sadournay (1972):

2. **Equiangular** (Ronchi, 1995), most common, used by LFRic (UK Metoffice), SE (NCAR)

- Equal angles on the sphere = more uniform cells

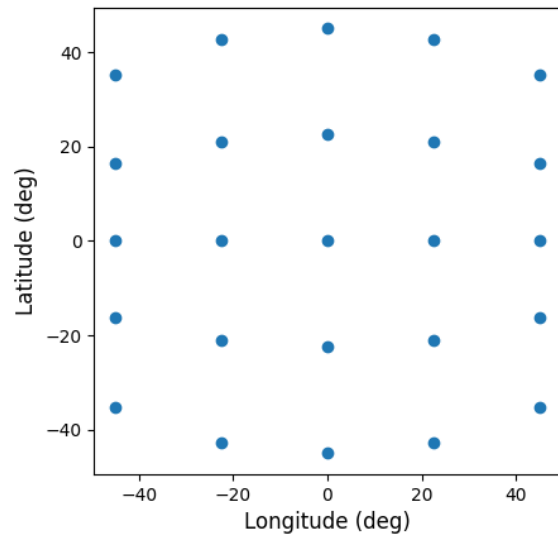
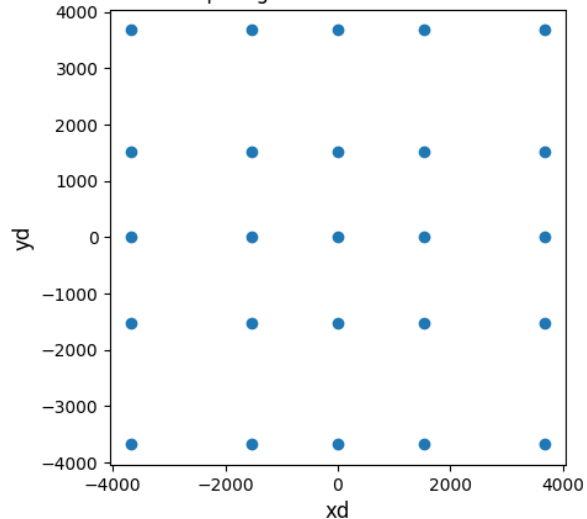
3. **Equi-edge**, an additional option (default) for FV3



Local panel

Map

On the sphere



# Three cubed-sphere grids

## 1. **Equidistant**, original grid of Sadournay (1972):

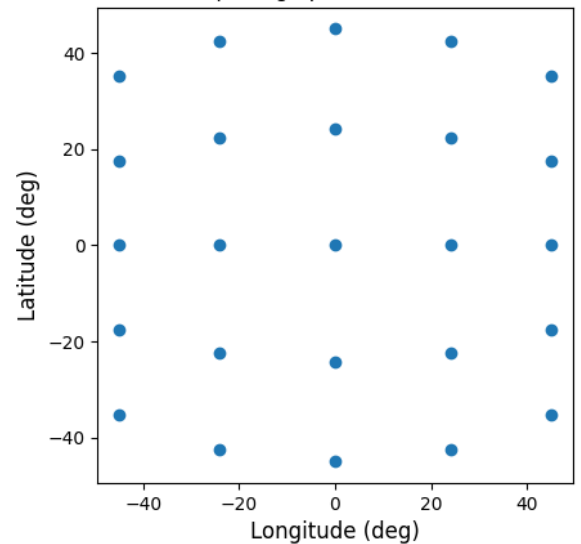
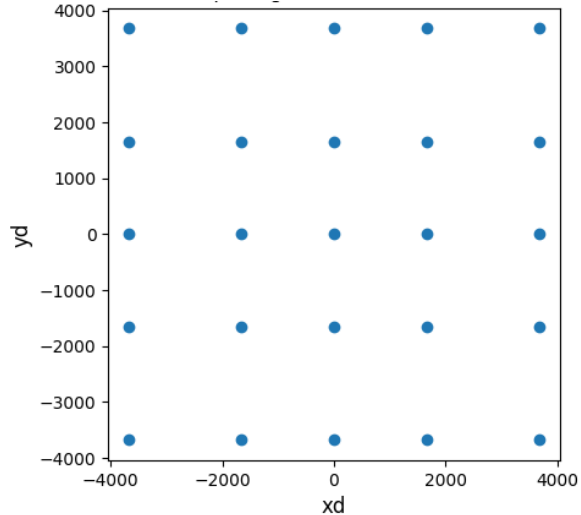
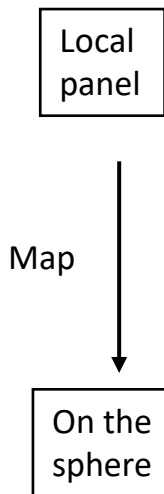
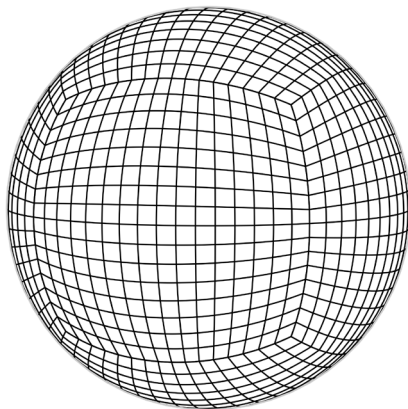
- Equal spacings on the local panel  
= wide range of cell areas

## 2. **Equiangular** (Ronchi, 1995), most common, used by LFRic (UK Metoffice), SE (NCAR)

## 3. **Equi-edge**, an additional option (default) for FV3

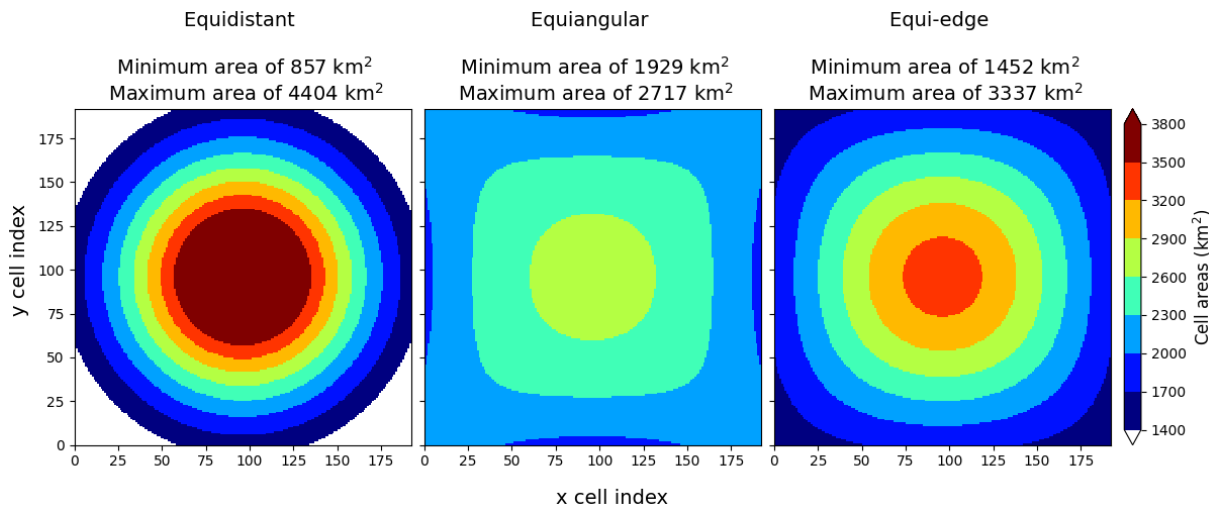
- More uniform cells at panel edges

See Santos (2024) thesis for more details on these grids.



# Comparison of cubed-sphere grids:

	Equidistant	Equiangular	Equi-edge
Range of cell areas	Largest	Smallest	
Location of smallest cell	Corners	Middle of edges	Corners
Maximum aspect ratio ( $\Delta y/\Delta x$ )	$1.41 (\sqrt{2})$	$1.41 (\sqrt{2})$	$\sim 1.06$



# Contents:

1. Divergence and vorticity damping
2. Cubed-sphere grids
3. Linear stability analysis
4. Application to CAM-FV3

Details of the linear stability analysis are found in ARXIV pre-print: *Stability analyses of divergence and vorticity damping on gnomonic cubed-sphere grids*, Andrews and Jablonowski (2025).



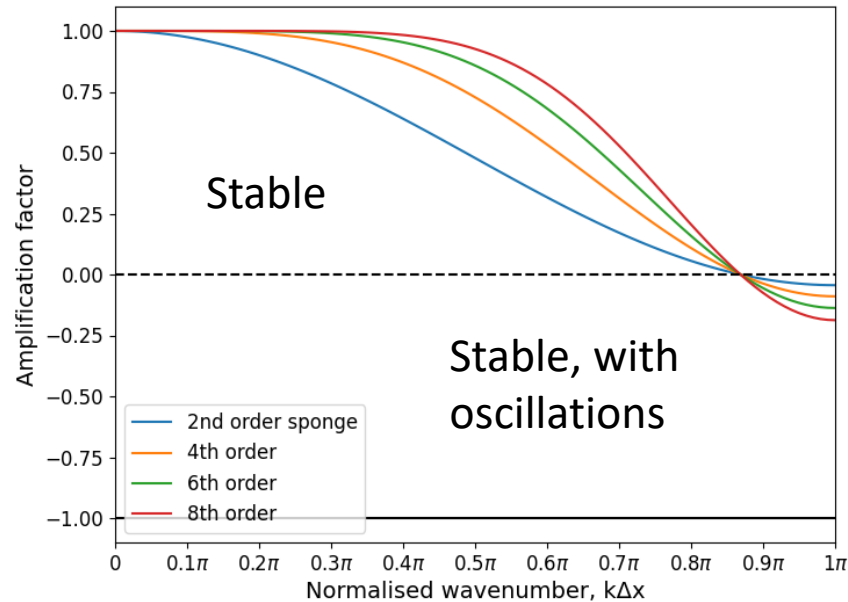
# Amplification factors

$$\Gamma = e^{i\omega\Delta t}$$

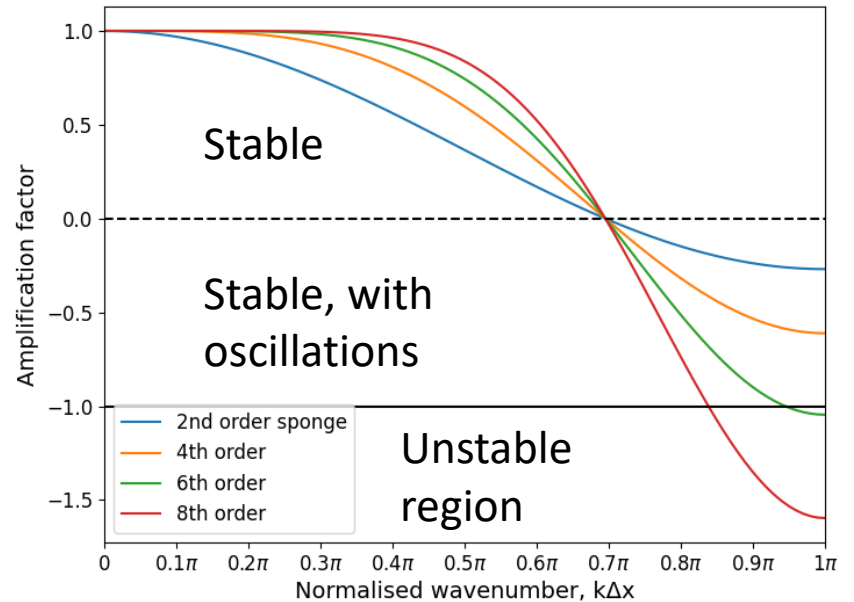
CAM defaults: Laplacian  $C_{D,2} = 0.15$  in the upper sponge, hyperviscous  $C_{D,2q} = 0.15$

Equi-edge is stable. 6<sup>th</sup> and 8<sup>th</sup> order equiangular are **unstable**.

Equi-edge



Equiangular



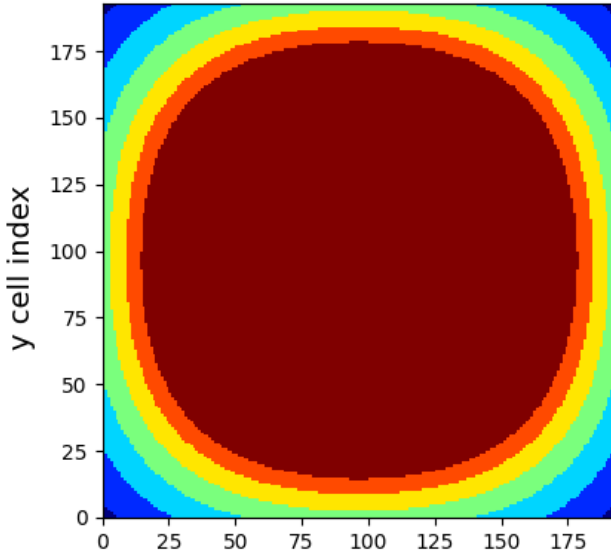
# Grid stability function

$$C_{D,2q} \leq 2^{1/q} \frac{\Psi_{c,\min}}{4}$$

Minimum  $\Psi_c$  for equi-edge is  $\sim 1.22 \left(\sqrt{2/3}\right)$  greater than equiangular

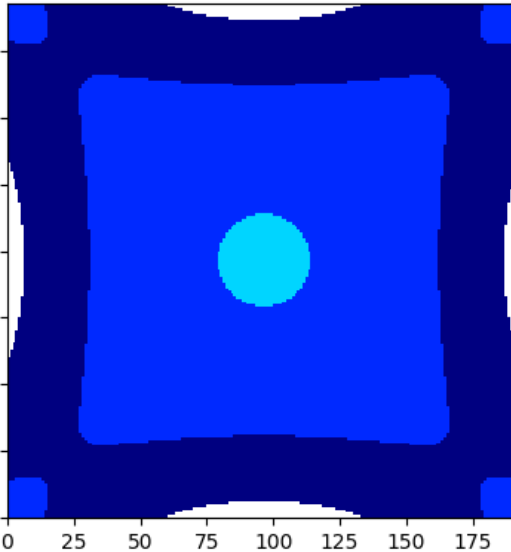
Equidistant

Minimum value of  $\Psi$  is 0.577



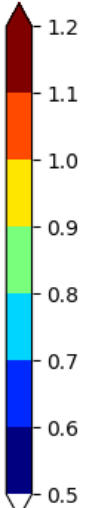
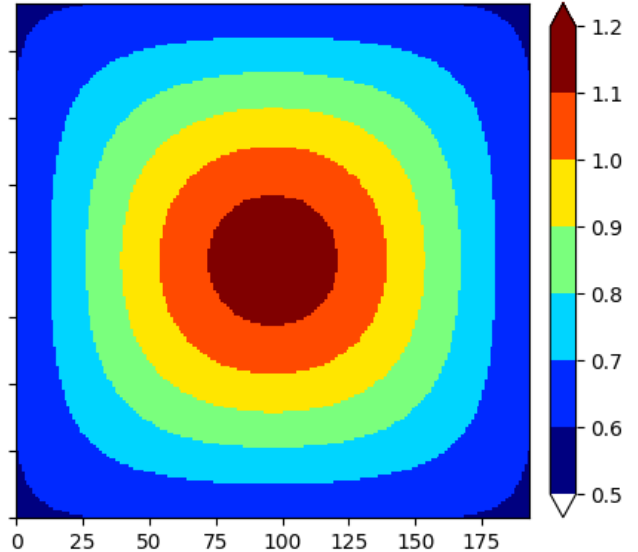
Equiangular

Minimum value of  $\Psi$  is 0.471



Equi-edge

Minimum value of  $\Psi$  is 0.577



Corners

Middle of edges

Corners

# CAM-FV3 testing

- Use the baroclinic wave test case of Jablonowski, Williamson (2006)
- Run for fifteen days and identify the largest stable  $C_{D,2q}$
- Equi-edge and equiangular grids

# CAM-FV3\* horizontal momentum equations

$$\frac{\partial u}{\partial t} = (Y + \mathcal{V}_{y,2q}) + \dots + \delta_x \mathcal{D}_x,$$

$$\frac{\partial v}{\partial t} = -(X + \mathcal{V}_{x,2q}) + \dots + \delta_x \mathcal{D}_y,$$

- $X, Y$  transport operators implicitly diffuse  $\xi$  but not  $D$
- $\mathcal{D}$  are divergence damping terms (required)
- $\mathcal{V}$  are vorticity damping terms (optional)

\* CAM-FV3: NCAR Community Atmosphere Model (CAM), run with the finite-volume cubed-sphere (FV3) dynamical core.

# CAM-FV3 divergence damping

$$\frac{\partial u}{\partial t} = (Y + \mathcal{V}_{y,2q}) + \dots + \delta_x \mathcal{D}_x,$$

$$\frac{\partial v}{\partial t} = -(X + \mathcal{V}_{x,2q}) + \dots + \delta_x \mathcal{D}_y,$$

- $X, Y$  transport operators implicitly diffuse  $\xi$  but not  $D$
- $\mathcal{D}$  are divergence damping terms (required)
- $\mathcal{V}$  are vorticity damping terms (optional)

# Divergence damping in CAM-FV3

	Equi-edge				Equiangular			
	2nd	4th	6th	8th	2nd	4th	6th	8th
Linear stability limit	0.289	0.204	0.182	0.172	0.236	0.167	0.148	0.140
Default CAM (monotonic), C192	0.291	0.204	0.182	0.172	0.239	0.169	0.151	0.142
Virtually-inviscid unlimited, C192	0.285	0.200	0.180	0.170	0.234	0.167	0.149	None

- Equi-edge can use stronger divergence damping.

# Divergence damping in CAM-FV3

	Equi-edge				Equiangular			
	2nd	4th	6th	8th	2nd	4th	6th	8th
Linear stability limit	0.289	0.204	0.182	0.172	0.236	0.167	0.148	0.140
Default CAM (monotonic), C192	0.291	0.204	0.182	0.172	0.239	0.169	0.151	0.142
Virtually-inviscid unlimited, C192	0.285	0.200	0.180	0.170	0.234	0.167	0.149	None

- Equi-edge can use stronger divergence damping.
- Equiangular sixth- and eighth-orders are unstable with CAM default  $C_D = 0.15$ .

# Divergence damping blow-up locations

OMEGA850: Vertical pressure velocity (Pa/s) at 850 hPa.

Using 6<sup>th</sup>-order divergence damping with  $C_{D,6}$  0.001 above the stable value.

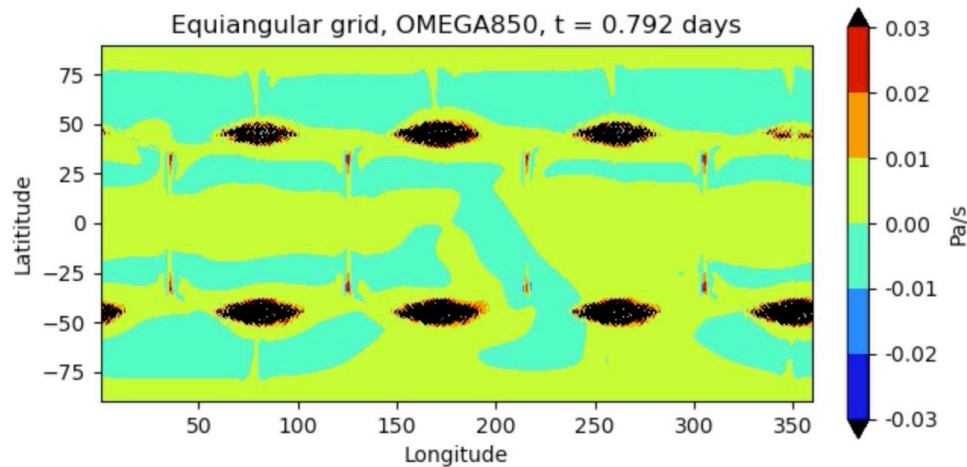
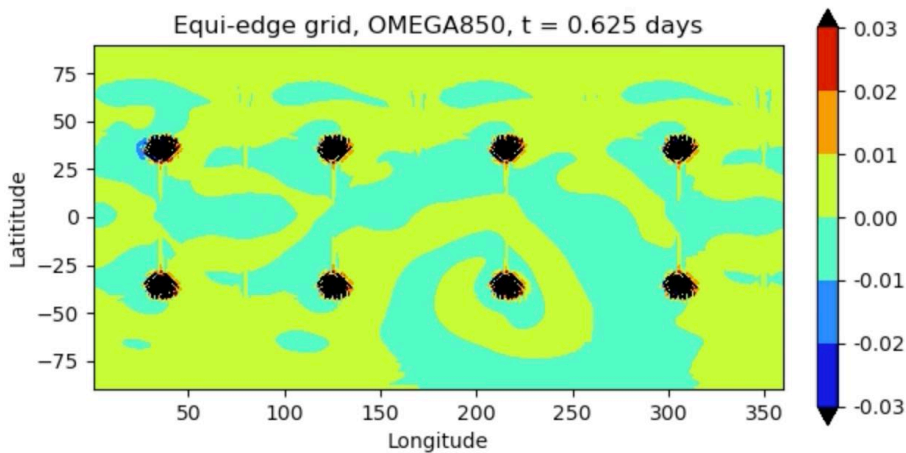




# Divergence damping blow-up locations

OMEGA850: Vertical pressure velocity (Pa/s) at 850 hPa.

Using 6<sup>th</sup>-order divergence damping with  $C_{D,6}$  0.001 above the stable value.



# CAM-FV3 vorticity damping

$$\frac{\partial u}{\partial t} = (Y + \mathcal{V}_{y,2q}) + \dots + \delta_x \mathcal{D}_x,$$

$$\frac{\partial v}{\partial t} = -(X + \mathcal{V}_{x,2q}) + \dots + \delta_x \mathcal{D}_y,$$

- $X, Y$  transport operators implicitly diffuse  $\xi$  but not  $D$
- $\mathcal{D}$  are divergence damping terms (required)
- $\mathcal{V}$  are vorticity damping terms (optional)

# Vorticity damping in CAM-FV3

1. Vorticity limits are well below linear theory, due to implicit transport diffusion.

	Equi-edge			
Grid resolution	C96		C192	
Diffusion order	4th	6th	4th	6th
Theoretical	0.203	0.181	0.204	0.181
Default CAM (monotonic)	0.099	0.114	0.090	0.107

# Vorticity damping in CAM-FV3

1. Vorticity limits are well below linear theory, due to implicit transport diffusion.
2. Sixth-order has a larger stability range than fourth-order.

Grid resolution	Equi-edge			
	C96		C192	
Diffusion order	4th	6th	4th	6th
Theoretical	0.203	0.181	0.204	0.181
Default CAM (monotonic)	0.099	0.114	0.090	0.107

# Vorticity damping in CAM-FV3: The transport scheme affects stability

3. Maximum  $C_{\xi,2q}$  depends on the horizontal transport scheme.

Monotonic = more constraints, generally more diffusive.

Grid resolution	Equi-edge			
	C96		C192	
Diffusion order	4th	6th	4th	6th
Theoretical	0.203	0.181	0.204	0.181
Lin monotonic	0.097	0.113	0.087	0.104
Intermediate unlimited	0.098	0.113	0.089	0.106
Default CAM (monotonic)	0.099	0.114	0.090	0.107
Virtually-inviscid unlimited	0.104	0.116	0.094	0.108
Huynh monotonic	0.105	0.119	0.098	0.113

**Hypothesis: Can this indicate the implicit diffusion from transport?**

# Key Conclusions

- Equi-edge can use stronger divergence damping than equiangular
  - CAM-FV3 defaults are unstable for equiangular (sixth- and eighth-orders)!

# Conclusions

- Equi-edge can use stronger divergence damping than equiangular
  - CAM-FV3 defaults are unstable for equiangular (sixth- and eighth-orders)!
- Different blow-up locations on the two grids:
  - Equi-edge at panel corners
  - Equiangular at the centre of panel edges

# Conclusions

- Equi-edge can use stronger divergence damping than equiangular
  - CAM-FV3 defaults are unstable for equiangular (sixth- and eighth-orders)!
- Different blow-up locations on the two grids:
  - Equi-edge at panel corners
  - Equiangular at the centre of panel edges
- The maximum stability of vorticity damping depends on the transport scheme
  - Can this indicate implicit diffusion?



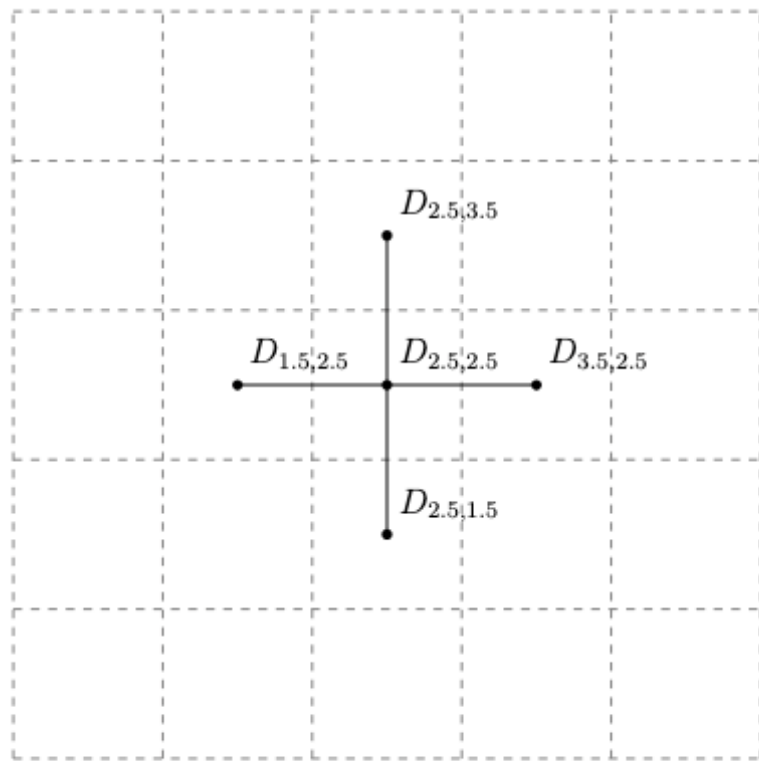
# Conclusions

- Equi-edge can use stronger divergence damping than equiangular
  - CAM-FV3 defaults are unstable for equiangular (sixth- and eighth-orders)!
- Different blow-up locations on the two grids:
  - Equi-edge at panel corners
  - Equiangular at the centre of panel edges
- The maximum stability of vorticity damping depends on the transport scheme
  - Can this indicate implicit diffusion?
- ARXIV pre-print: *Stability analyses of divergence and vorticity damping on gnomonic cubed-sphere grids, Andrews and Jablonowski (2025).*

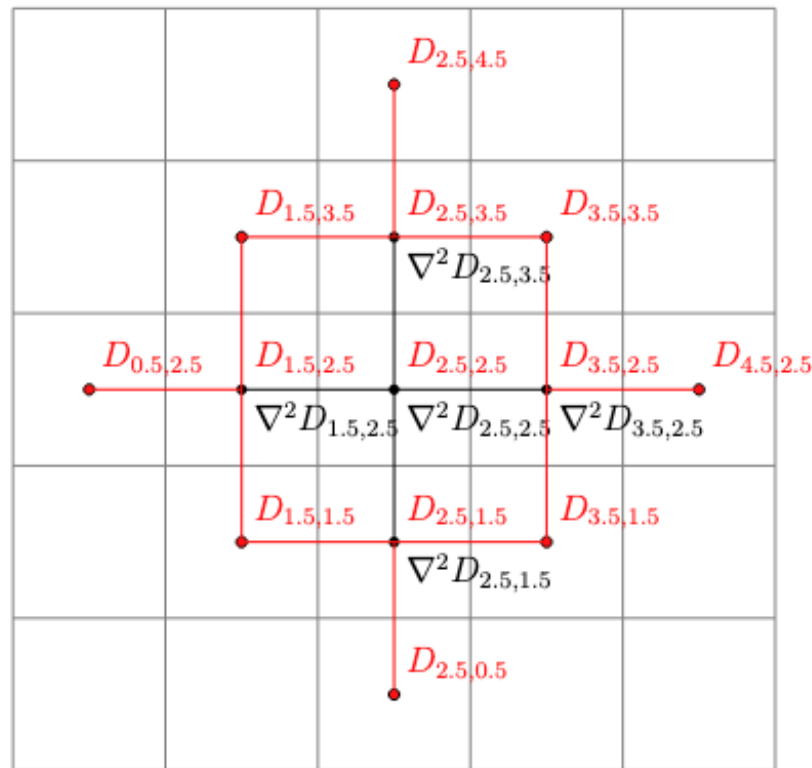
ADDITIONAL SLIDES

# Stencils

A higher order of damping requires more ghost cells.



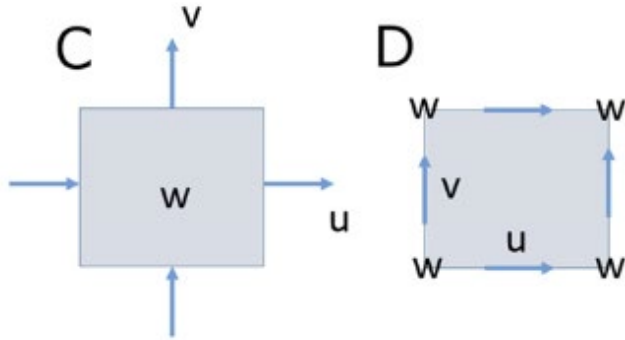
(a) Stencil for Laplacian divergence damping



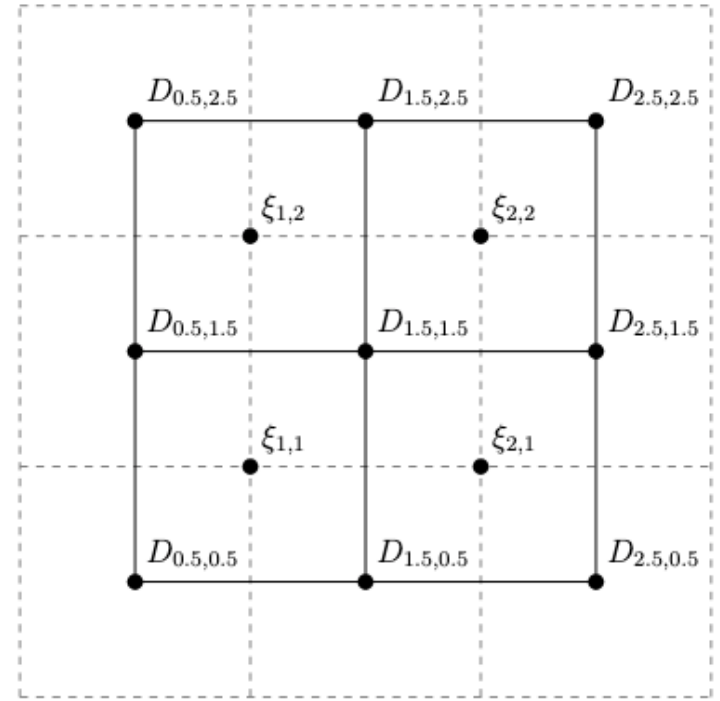
(b) Stencil for fourth-order divergence damping

# C- and D-grids

- For application to CAM-FV3, we use the D-grid.
- For the C-grid, the  $C_D$ ,  $C_\xi$  limits are swapped.



Pletzer, Hayek (2018)



————— D-grid

- - - - - C-grid

# Linear stability

- Introduce a grid stability function:

$$\Psi_c(x, y) = \frac{\Delta A_c}{\sin(\alpha)\Delta A_{\min}(\chi + \chi^{-1})}$$

- Then, the linear stability limit is:

$$C_{D,2q} \leq 2^{1/q} \frac{\Psi_{c,\min}}{4}$$

- For vorticity damping, D-grid evaluations are used:

$$C_{\xi,2q} \leq 2^{1/q} \frac{\Psi_{d,\min}}{4}$$

- $\Delta A_c$  cell areas on the cubed-sphere
- $\sin(\alpha)$  is internal angle; quantifies non-orthogonality

- $\Delta A_{\min}$  the smallest cell area
- $\chi = \frac{\Delta y}{\Delta x}$  is the cell aspect ratio

# Grid stability function

Minimum value for the equi-edge grid:  $\frac{1}{\sqrt{3}} \approx 0.577$

Minimum value for the equiangular grid:  $\frac{\sqrt{2}}{3} \approx 0.471$

Ratio is  $\sqrt{\frac{2}{3}} \approx 1.22$

There is a larger range of stable coefficients on the equi-edge grid.

$$C_{D,2q} \leq 2^{1/q} \frac{\Psi_{c,\min}}{4}$$

# Divergence damping in CAM-FV3

Compare five transport schemes:

Two unlimited, three monotonic.

	Equi-edge				Equiangular			
	2nd	4th	6th	8th	2nd	4th	6th	8th
Linear stability limit	0.289	0.204	0.182	0.172	0.236	0.167	0.148	0.140
Default CAM (monotonic), C96	0.295	0.206	0.184	0.174	0.242	0.171	0.153	0.144
Lin monotonic, C96	0.295	0.206	0.184	0.174	0.241	0.171	0.152	0.144
Huynh monotonic, C96	0.294	0.206	0.184	0.174	0.242	0.171	0.153	0.144
Virtually-inviscid unlimited, C96	0.296	0.203	0.183	0.173	0.241	0.169	0.151	0.143
Intermediate unlimited, C96	0.291	0.203	0.182	0.173	0.242	0.171	0.152	0.144
Default CAM (monotonic), C192	0.291	0.204	0.182	0.172	0.239	0.169	0.151	0.142
Virtually-inviscid unlimited, C192	0.285	0.200	0.180	0.170	0.234	0.167	0.149	None

# Mixed-order divergence damping

$$\frac{\partial D}{\partial t} = \dots + \nu_{D,2} \nabla^2 D + (-1)^{q+1} \nu_{D,2q} \nabla^{2q} D$$

Fix Laplacian coefficient,  $C_{D,2} = 0.05$ , then find maximum  $C_{D,2q}$

Single-order	Equi-edge				Equiangular			
	2nd	4th	6th	8th	2nd	4th	6th	8th
Linear stability limit	0.289	0.204	0.182	0.172	0.236	0.167	0.148	0.140
Default CAM (monotonic), C96	0.295	0.206	0.184	0.174	0.242	0.171	0.153	0.144

Mixed-order	Equi-edge			Equiangular		
Additional hyperviscosity order	4th	6th	8th	4th	6th	8th
Linear stability limit	0.185	0.171	0.164	0.148	0.137	0.132
Default CAM (monotonic)	0.185	0.171	0.164	0.150	0.139	0.134



	Equi-edge				Equiangular			
Grid resolution	C96		C192		C96		C192	
Diffusion order	4th	6th	4th	6th	4th	6th	4th	6th
Theoretical	0.203	0.181	0.204	0.181	0.167	0.149	0.167	0.149
Lin monotonic	0.097	0.113	0.087	0.104	0.110	0.113	0.107	0.111
Intermediate unlimited	0.098	0.113	0.089	0.106	0.110	0.113	0.107	0.111
Default CAM (monotonic)	0.099	0.114	0.090	0.107	0.110	0.113	0.107	0.111
Virtually-inviscid unlimited	0.104	0.116	0.094	0.108	0.110	0.113	0.107	0.111
Huynh monotonic	0.105	0.119	0.098	0.113	0.110	0.113	0.107	0.111

# Computing $\sin(\alpha)$

$$\hat{\mathbf{e}}_{ij} = \frac{\mathbf{p}_i \times \mathbf{p}_j}{\|\mathbf{p}_i \times \mathbf{p}_j\|}.$$

$$\alpha_{jik} = \arccos(\hat{\mathbf{e}}_{ij} \cdot \hat{\mathbf{e}}_{ik}).$$

$$\alpha = \frac{1}{4}(\alpha_{412} + \alpha_{123} + \alpha_{234} + \alpha_{341}).$$

